

New Superheavy Element Isotopes: $^{242}\text{Pu}(^{48}\text{Ca}, 5n)^{285}114$

P. A. Ellison,^{1,2} K. E. Gregorich,² J. S. Berryman,² D. L. Bleuel,³ R. M. Clark,² I. Dragojević,² J. Dvorak,⁴ P. Fallon,² C. Fineman-Sotomayor,^{1,2} J. M. Gates,² O. R. Gothe,^{1,2} I. Y. Lee,² W. D. Loveland,⁵ J. P. McLaughlin,^{1,2} S. Paschalis,² M. Petri,² J. Qian,² L. Stavsetra,⁶ M. Wiedeking,³ and H. Nitsche^{1,2}

¹Department of Chemistry, University of California, Berkeley, California 94720, USA

²Lawrence Berkeley National Laboratory, Berkeley, California 94720, USA

³Lawrence Livermore National Laboratory, Livermore, California 94550, USA

⁴GSI Helmholtzzentrum für Schwerionenforschung, GmbH, 64550 Darmstadt, Germany

⁵Department of Chemistry, Oregon State University, Corvallis, Oregon 97331, USA

⁶Institute for Energy Technology, N-2007 Kjeller, Norway

(Received 23 July 2010; published 26 October 2010)

The new, neutron-deficient, superheavy element isotope $^{285}114$ was produced in ^{48}Ca irradiations of ^{242}Pu targets at a center-of-target beam energy of 256 MeV ($E^* = 50$ MeV). The α decay of $^{285}114$ was followed by the sequential α decay of four daughter nuclides, ^{281}Cn , ^{277}Ds , ^{273}Hs , and ^{269}Sg . ^{265}Rf was observed to decay by spontaneous fission. The measured α -decay Q values were compared with those from a macroscopic-microscopic nuclear mass model to give insight into superheavy element shell effects. The $^{242}\text{Pu}(^{48}\text{Ca}, 5n)^{285}114$ cross section was $0.6^{+0.9}_{-0.5}$ pb.

DOI: 10.1103/PhysRevLett.105.182701

PACS numbers: 25.70.Gh, 23.60.+e, 25.85.Ca, 27.90.+b

Superheavy element (SHE) formation by compound nucleus reactions between ^{48}Ca ion beams and actinide targets have recently been shown to occur with picobarn-level cross sections [1–4]. The products of these reactions include six new elements and 46 new isotopes. In the present work, the Berkeley Gas-Filled Separator (BGS) at the Lawrence Berkeley National Laboratory (LBNL) 88-Inch Cyclotron was used to extend the region of enhanced stability consisting of nuclides produced by ^{48}Ca irradiations of actinide targets along its neutron-deficient edge by studying the $^{242}\text{Pu}(^{48}\text{Ca}, 5n)^{285}114$ reaction.

The production of element 114 by bombarding ^{242}Pu with ^{48}Ca was first observed by Oganessian *et al.* [5]. In that study, $^{290}114^*$ compound nuclei were produced with several different excitation energies E^* with a maximum of $E^* = 45$ MeV, resulting in the observation of the three-neutron ($3n$) and four-neutron ($4n$) evaporation products. While ^{242}Pu was never reported to be irradiated at energies high enough to maximize the $5n$ evaporation product, Oganessian *et al.* did perform irradiations of ^{244}Pu with ^{48}Ca with E^* up to 53 MeV [6]. At this excitation energy, one event of the $5n$ product, $^{287}114$, was observed. In the ^{244}Pu irradiations, the observed cross section for the $5n$ reaction was $1.1^{+2.6}_{-0.9}$ pb, which, although agreeing within error bars, was 2 times larger than theoretical predictions by Zagrebaev [7]. Zagrebaev predicts a maximum cross section of 0.3 pb for the $^{242}\text{Pu}(^{48}\text{Ca}, 5n)^{285}114$ reaction discussed in this work [8].

Based on extrapolations of experimental masses [9], standard α -decay systematics [10], and predictions of spontaneous-fission (SF) half-lives [11], $^{285}114$ is predicted to decay through a series of α decays until the SF

of ^{265}Rf , resulting in a total of six previously undiscovered isotopes. Analysis of the α -decay energies of the new isotopes provides insight into the accuracy of modern predictions of the shell structure of the heaviest elements. In addition, these isotopes would be the most neutron-deficient even- Z isotopes observed in ^{48}Ca bombardments of actinide targets.

The LBNL Advanced Electron Cyclotron Resonance ion source [12] was used to produce beams of $^{48}\text{Ca}^{11+}/^{10+}$. The 88-Inch Cyclotron accelerated the ^{48}Ca to 273 MeV with typical intensities of 300 particle nanoamperes. A total beam dose of 3.1×10^{18} ^{48}Ca ions was delivered over 22.8 effective days of irradiation. At the entrance to the BGS, the ion beam passed through a $45 \mu\text{g}/\text{cm}^2$ carbon window separating beam line vacuum from the 67-Pa He gas inside. The beam then passed through the titanium target backing foil followed by the $^{242}\text{PuO}_2$ target material. Targets were prepared by electrodeposition from isopropanol solutions. Four target segments with 440, 340, 320, and 270 $\mu\text{g}/\text{cm}^2$ of ^{242}Pu ($> 99\%$ purity) on 2.4- μm Ti backing foils were mounted on a 9.5-cm diameter wheel. The energy loss in the entrance window and targets was calculated using SRIM2003 [13]. The four target segments had calculated center-of-target beam energies of 255.5, 256.0, 256.1, and 256.3 MeV, respectively, with target thickness weighted average center-of-target beam energy of 255.9 MeV and compound nucleus excitation energy of 50.1 MeV [9,14]. The systematic error in the cyclotron beam energy is 1%. The ^{48}Ca ion beam lost 2.5–4.1 MeV upon passing through the $^{242}\text{PuO}_2$ target layer. The target wheel was rotated at ~ 12 Hz to disperse the heat of the beam. Elastically scattered ^{48}Ca ions were recorded by a silicon p - i - n detector mounted 27° from the beam axis and

used to monitor the product of beam dose and target thickness.

Compound nucleus evaporation residues (EVRs) recoiled from the target with the momentum of the beam. The BGS separated these from unreacted beam and other reaction products by their differing magnetic rigidities in helium. The transmission efficiency for an EVR to reach the focal plane detector was calculated using a Monte Carlo simulation of trajectories through the BGS combined with experimentally measured efficiencies. The calculated efficiency for $^{285}\text{114}$ EVRs was 69%.

In the focal plane area of the BGS, EVRs traveled through a multiwire proportional counter (MWPC) filled with 370-Pa isobutane before implanting in the focal plane detector (FPD). Analog signals from the MWPC were used along with the time of flight between the MWPC and FPD to distinguish implantation events from radioactive decay events in the FPD. The FPD consisted of silicon detectors with a total of 48 vertical strips that provided horizontal position resolution. Vertical position was measured by resistive charge division within each strip and reported as the distance from the vertical center of the detector. Error in this position was experimentally determined to be $\sigma_y(E_{\text{FPD}}) = 2600 \text{ (keV} \cdot \text{mm)} / E_{\text{FPD}}$ for the energy range of α particles. Events depositing less than 2 MeV in the FPD had an additional vertical position uncertainty due to integral nonlinearity in the low end of the analog-to-digital converter (ADC) range. Because fission energies were measured in a separate set of amplifiers and ADCs, 1.5 mm was added to the vertical position uncertainty for fission events. Additional silicon chips were located upstream and perpendicular to the FPD forming a five-sided box configuration. These so-called “upstream detectors” (UDs) allowed for the reconstruction of α decay and fission events that only deposited partial energy in the FPD. The overall efficiency was approximately 75% for detecting full-energy α particles (either entirely in the FPD or FPD-UD reconstructed) and 100% for detecting at least one fragment from a SF decay of an implanted atom. A silicon punchthrough detector was mounted immediately behind the FPD to detect and veto events from low-ionizing particles passing through the 300- μm -thick FPD. A standard high-purity germanium clover detector [15] was mounted behind a 2-mm-thick aluminum vacuum window directly behind the FPD. The efficiency for detecting superheavy element x rays was approximately 13% for an assumed recoil distribution centered on the FPD.

Element-114 atoms were identified by detecting time- and position-correlated events corresponding to their implantation and subsequent radioactive decay chain, terminating with the detection of a SF event. Table I contains the times, energies, and positions of the two correlated decay chains observed in the experiment. Based on a comparison with predicted decay properties, the first event was assigned to the decay of $^{285}\text{114}$ and its daughters. This decay chain consisted of a 15.97 MeV EVR-like event

TABLE I. Observed element-114 decay chains.

Interpretation	E (MeV)	Δt (s)	Pos (mm)
EVR—strip 28	15.97(4)		−1.0(2)
$^{285}\text{114}$ α decay	1.64(10) ^a	0.181	1.2(16)
^{281}Cn α decay	10.31(4)	0.140	−0.8(3)
^{277}Ds α decay	10.57(4)	0.008 21	−0.9(2)
^{273}Hs α decay	9.59(4)	0.346	−0.9(3)
^{269}Sg α decay	8.57(10) ^b	185	1.2(33)
^{265}Rf SF decay	208.1	152	−1.1(15)
EVR—strip 16	14.37(4)		−24.8(2)
$^{286}\text{114}$ α decay	10.31(10) ^c	0.0760	−20.4(39)
^{282}Cn SF decay	205.4	0.000 522	−22.5(15)

^aEscape α particle depositing only partial energy in FPD.

^bReconstructed: 0.742 MeV in FPD and 7.823 MeV in UD.

^cReconstructed: 0.600 MeV in FPD and 9.705 MeV in UD.

[$5 < E(\text{MeV}) < 18$, FPD only, anticoincident with punchthroughs, coincident with MWPC] followed 0.181 s later by a 1.64 MeV escapelike event [$0.5 < E(\text{MeV}) < 2$, FPD only, anticoincident with punchthroughs and MWPC] indicative of an α -decay event in which the α particle escaped from the front of the five-sided detector box. The chain continued with four subsequent α -like events [$8 < E(\text{MeV}) < 12$, FPD only or FPD-UD reconstructed, anticoincident with punchthroughs and MWPC] after 140 ms, 8.21 ms, 346 ms, and 185 s with energies of 10.31, 10.57, 9.59, and 8.57 MeV, which are interpreted as the successive α decays of $^{281}_{112}\text{Cn}$, $^{277}_{110}\text{Ds}$, $^{273}_{108}\text{Hs}$, and $^{269}_{106}\text{Sg}$, respectively. The final α -like event in this chain was reconstructed from a 0.742 MeV signal in the FPD and a 7.823 MeV signal in the UD. The decay chain terminated 152 seconds later with a 208.1 MeV SF-like event [$E(\text{MeV}) > 80$, FPD only or FPD-UD reconstructed, anticoincident with punchthroughs and MWPC] interpreted as the SF of $^{104}_{265}\text{Rf}$. The vertical positions of the events in this chain agree well. As the first detected full-energy α -like event is similar in energy and lifetime to the decay of $^{286}\text{114}$, one may postulate that the 1.64-MeV event was a random correlation and the decay chain was that of $^{286}\text{114}$ decaying through a previously unobserved α branch of ^{282}Cn . We do not believe this is the case because (i) based on the random rate of escapelike events, the probability that we would observe a randomly correlated event in the 0.32 s between the recoil and first α -like event was 0.0070, (ii) the observed lifetime for the event that would be assigned to the α decay of ^{282}Cn was 10 times the published half-life for the nuclide [1], and (iii) SF was observed for all of the previous observations of ^{282}Cn [1,3].

The second observed decay chain was assigned to the decay of $^{286}\text{114}$ and ^{282}Cn . The chain consisted of a 14.37 MeV EVR-like event followed 76 ms later by a 10.31 MeV α -like event which was reconstructed from 0.600 MeV in the FPD and 9.705 MeV in the UD. A 205.4 MeV SF-like event occurred 0.52 ms later. The decay energies and lifetimes of this event agreed very well with

the published decay properties of $^{286}114$ [1] ($t_{1/2} = 0.13$ s; 50% 10.19 MeV α decay, 50% SF) and $^{282}114$ ($t_{1/2} = 0.82$ ms; 100% SF). The SF-like events for both decay chains were each observed with two coincident γ rays, reinforcing their assignments as SF events. No γ rays were observed coincident with any of the correlated α - or escapelike events.

The numbers of expected decay chains made from coincidences of unrelated events matching the decay properties of $^{285}114$ or $^{286}114$ were estimated. To simplify the calculation, we assumed all events were evenly distributed over the FPD and the rates were constant at their average values. During the experiment, the rate of EVR-like events for the whole array was 0.38 Hz and the rate of α -like events was 0.011 Hz. A total of 9 SF-like events were observed [only 3 with $E(\text{MeV}) > 101$]. The number of expected random $^{285}114$ -like decay chains was calculated by multiplying the 9 SF-like events by the probability that they were correlated within 20 h to at least one EVR-like and three α -like events with the additional requirement that at least one of the α lifetimes was less than 3 s. Using this very general schematic of a $^{285}114$ -like event, the number of random correlations was calculated to be 9.2×10^{-4} . The number of random $^{286}114$ -like event chains with an EVR-like event followed by an α -like event and a SF-like event within 10 times the published half-lives (1.3 s for 0.13-s $^{286}114$ and 8.2 ms for 0.82-ms $^{282}114$) was calculated to be 1.7×10^{-9} . These simplified overestimations do not consider event order or α -decay systematics [10]. Because these numbers are very low, it is unlikely that either of the event chains were attributable to a random correlation of unrelated events.

Figure 1 shows theoretical predictions [7,8] and experimental measurements [1,3] of excitation functions for the

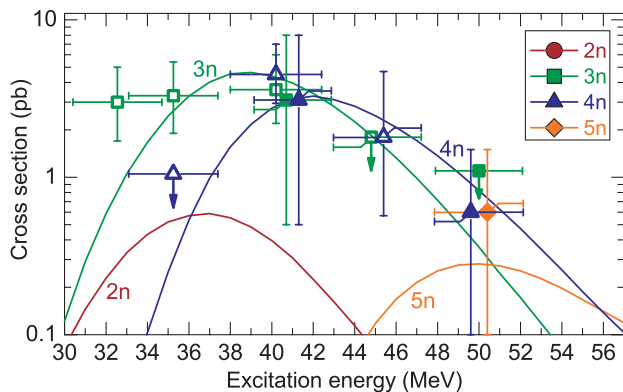


FIG. 1 (color online). Overview of experimental measurements and theoretical predictions for the excitation functions of the $^{242}\text{Pu}(^{48}\text{Ca}, 2-5n)^{288-285}114$ nuclear reactions. Theoretical predictions from [7,8] are shown as colored curves. Experimental cross sections for the 3n (green squares), 4n (blue triangles), and 5n (orange diamonds) reactions measured at the BGS (solid symbols) at 41 MeV [3], from the current work at 50 MeV, and from [1] (open symbols) at 32.5, 35.3, 40.2, and 45.1 MeV, are shown.

$^{242}\text{Pu}(^{48}\text{Ca}, 2-5n)^{285-288}114$ reactions. The cross sections measured at the compound nucleus excitation energy $E^* = 50$ MeV for the 4n and 5n products in this work are $0.6^{+0.9}_{-0.5}$ pb, each. Error bars are a 68% confidence interval with minimal length and highest probability density calculated according to the methods of Brüche [16]. The nonobservation of a 3n evaporation product gave an 84% confidence upper limit for the $^{242}\text{Pu}(^{48}\text{Ca}, 3n)^{287}114$ reaction of 1.1. This cross section measured for the 5n reaction is larger than Zagrebaev's predictions [8] by a factor of 2, although agreeing within error bars. As a similar experimental-theoretical cross section discrepancy was observed for the $^{244}\text{Pu}(^{48}\text{Ca}, 5n)^{287}114$ reaction [6], it is possible that the predictions by Zagrebaev are systematically underestimating the 5n cross section, although current data cannot say so with statistical certainty. The measured element-114 magnetic rigidities were 2.26(3) and 2.31(3) Tm for the $^{285}114$ and $^{286}114$ events, respectively, and consistent with the 2.28 Tm value reported in [4]. The 3n and 4n cross section values measured at $E^* = 41$ MeV in 2009 at the BGS [3] were adjusted from $1.4^{+3.2}_{-1.2}$ pb to $3.1^{+4.9}_{-2.6}$ pb after taking into account an element-114 EVR magnetic rigidity of 2.28 Tm and magnetic field saturation in the second dipole magnet of BGS. This reassessed cross section is in good agreement with the cross sections measured by Oganessian *et al.* and theoretical predictions (see Fig. 1).

Figure 2 compares theoretical prediction curves from Muntian *et al.* [17–19] with experimental measurements [20] of even- Z isotopes' α -decay Q values plotted against their number of neutrons. Predicted neutron shell closures appear as local minima in the curves. Predicted proton shell closures appear as larger gaps between subsequent even- Z isotope curves. A detailed ground-state to ground-state Q value was unavailable for many of the odd- N experimental Q values including those of the current work. In these cases, the α -decay Q value was approximated by the recoil-corrected α -decay energy. Because the α -decay energy for $^{285}114$ was not observed, the recoil-corrected α -decay energy was deduced from the observed lifetime and α -decay systematics outlined by Parkhomenko and Sobiczewski [10]. By comparing the trend of discrepancies between experimental points and their theoretical counterparts, it is possible to evaluate how well the theoretical predictions model the shell effects that govern the stability of the transfermium elements. While the α -decay Q values measured in the current work agree well with predictions for Hs and Ds, the discrepancies in Sg, Cn, and element 114 highlight interesting deviations from the theoretical treatment of shell structure. First, the Q value measured for ^{269}Sg ($N = 163$) is significantly higher than predicted. Similarly, the α -decay Q value from ^{267}Sg ($N = 161$), of which one decay has been observed by Dvorak *et al.* [21,22], was measured to be above the predicted value. These observed discrepancies imply that the theory may overestimate the strength of

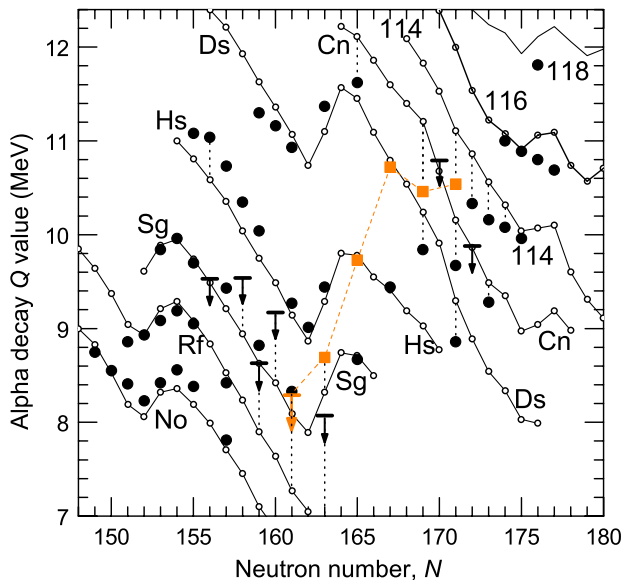


FIG. 2 (color online). Comparison of experimental and theoretical α -decay Q values versus neutron numbers for even- Z transfermium elements. Theoretical predictions from [17–19] are shown in small, connected, open points. Experimental data are shown in larger solid points. Data from the current work are shown as orange squares connected by dashed lines. 84% confidence upper limits are shown as horizontal lines for nuclides where only SF has been observed. Vertical dotted lines have been drawn to connect experimental points with their respective prediction curve when large deviations are present.

the $N = 162$ deformed shell closure for $Z = 106$ or underestimate it for $Z = 104$. Second, the α -decay Q values observed for ^{281}Cn ($N = 169$) and $^{285}114$ ($N = 171$) are significantly below their respective predicted values. This observation agrees well with the trend of other Cn and element-114 isotopes and may be either an experimental indication that the $Z = 114$ shell closure predicted around $N = 184$ extends to nuclides with neutron numbers significantly lower than predicted or a result of a systematic overestimation of α -decay Q values for nuclides with $169 < N < 174$. The observed spontaneous-fission lifetime of 152 s for ^{265}Rf is between the previously observed spontaneous-fission half-lives of neighboring odd- N isotopes ^{263}Rf ($t_{1/2} = 8$ s [21,22]) and ^{267}Rf ($t_{1/2} = 1.3$ h [1]).

The six new isotopes reported here are more neutron deficient than any previously observed even- Z superheavy element isotope [1–4]. Their discovery is an important step towards linking the six new superheavy elements and 52 new isotopes to the main body of the chart of nuclides. The successful bridging of this gap would provide a necessary proof for unambiguous proton- and neutron-number assignments for these new isotopes.

In summary, the LBNL 88-Inch Cyclotron was used to bombard ^{242}Pu targets with ^{48}Ca ion beams producing $^{290}114^*$ compound nuclei with an excitation energy of

50 MeV. Using the BGS, two decay chains were observed, one matching the predicted decay properties of $^{285}114$ and one matching the previously observed decay properties of $^{286}114$. The decay chain of $^{285}114$, which included a total of six new isotopes, was observed to α decay until the SF of ^{265}Rf . The isotopes observed in this decay chain are among the most neutron deficient produced in a ^{48}Ca irradiation of an actinide target. The observed α -decay Q values for the new isotopes were used to gain insight into the shell effects used in theoretical superheavy mass predictions.

The authors would like to thank the ion source staff and operators of the 88-Inch Cyclotron for providing reliable and intense ^{48}Ca ion beams as well as M. Cromaz and A. O. Macchiavelli for their assistance during the experiment. Financial support was provided by the Office of High Energy and Nuclear Physics, Nuclear Physics Division, and by the Office of Basic Energy Sciences, Division of Chemical Sciences, Geosciences and Biosciences of the U.S. Department of Energy, under Contract No. DE-AC02-05CH11231 and the National Nuclear Security Administration under Contracts No. DE-FC52-08NA28752 and No. DE-AC52-07NA27344.

- [1] Yu. Ts. Oganessian, *J. Phys. G* **34**, R165 (2007).
- [2] S. Hofmann *et al.*, *Eur. Phys. J. A* **32**, 251 (2007).
- [3] L. Stavsetra *et al.*, *Phys. Rev. Lett.* **103**, 132502 (2009).
- [4] Ch. E. Düllmann *et al.*, *Phys. Rev. Lett.* **104**, 252701 (2010).
- [5] Yu. Ts. Oganessian *et al.*, *Phys. Rev. C* **70**, 064609 (2004).
- [6] Yu. Ts. Oganessian *et al.*, *Phys. Rev. C* **69**, 054607 (2004).
- [7] V. I. Zagrebaev, *Nucl. Phys. A* **734**, 164 (2004).
- [8] V. I. Zagrebaev (private communication).
- [9] G. Audi, A. H. Wapstra, and C. Thibault, *Nucl. Phys. A* **729**, 337 (2003).
- [10] A. Parkhomenko and A. Sobczewski, *Acta Phys. Pol. B* **36**, 3095 (2005).
- [11] R. Smolańczuk, J. Skalski, and A. Sobczewski, *Phys. Rev. C* **52**, 1871 (1995).
- [12] Z. Q. Xie, *Rev. Sci. Instrum.* **69**, 625 (1998).
- [13] J. F. Ziegler, *Nucl. Instrum. Methods Phys. Res., Sect. B* **219–220**, 1027 (2004).
- [14] W. D. Myers and W. J. Świątecki, Lawrence Berkeley National Laboratory Report No. LBNL-36803, 1994; <http://ie.lbl.gov/txt/ms.txt>.
- [15] G. Duchêne *et al.*, *Nucl. Instrum. Methods Phys. Res., Sect. A* **432**, 90 (1999).
- [16] W. Bröchle, *Radiochim. Acta* **91**, 71 (2003).
- [17] I. Muntian, Z. Patyk, and A. Sobczewski, *Acta Phys. Pol. B* **32**, 691 (2001).
- [18] I. Muntian *et al.*, *Acta Phys. Pol. B* **34**, 2073 (2003).
- [19] I. Muntian, Z. Patyk, and A. Sobczewski, *Phys. At. Nucl.* **66**, 1015 (2003).
- [20] See supplementary material at <http://link.aps.org/supplemental/10.1103/PhysRevLett.105.182701> for details and references.
- [21] J. Dvorak *et al.*, *Phys. Rev. Lett.* **97**, 242501 (2006).
- [22] J. Dvorak *et al.*, *Phys. Rev. Lett.* **100**, 132503 (2008).